




Hippocampus and temporal pole functional connectivity is associated with age and individual differences in autobiographical memory

Roni Setton^{a,1} , Laetitia Mwilambwe-Tshilobo^b , Signy Sheldon^c, Gary R. Turner^d, and R. Nathan Spreng^{b,c,e,f,g,1} 

Edited by Marcus Raichle, Mallinckrodt Institute of Radiology and Department of Neurology, Washington University School of Medicine, St. Louis, MO; received February 18, 2022; accepted August 2, 2022

Recollection of one's personal past, or autobiographical memory (AM), varies across individuals and across the life span. This manifests in the amount of episodic content recalled during AM, which may reflect differences in associated functional brain networks. We take an individual differences approach to examine resting-state functional connectivity of temporal lobe regions known to coordinate AM content retrieval with the default network (anterior and posterior hippocampus, temporal pole) and test for associations with AM. Multiecho resting-state functional magnetic resonance imaging (fMRI) and autobiographical interviews were collected for 158 younger and 105 older healthy adults. Interviews were scored for internal (episodic) and external (semantic) details. Age group differences in connectivity profiles revealed that older adults had lower connectivity within anterior hippocampus, posterior hippocampus, and temporal pole but greater connectivity with regions across the default network compared with younger adults. This pattern was positively related to posterior hippocampal volumes in older adults, which were smaller than younger adult volumes. Connectivity associations with AM showed two significant patterns. The first dissociated connectivity related to internal vs. external AM across participants. Internal AM was related to anterior hippocampus and temporal pole connectivity with orbitofrontal cortex and connectivity within posterior hippocampus. External AM was related to temporal pole connectivity with regions across the lateral temporal cortex. In the second pattern, younger adults displayed temporal pole connectivity with regions throughout the default network associated with more detailed AMs overall. Our findings provide evidence for discrete ensembles of brain regions that scale with systematic variation in recollective styles across the healthy adult life span.

multiecho fMRI | cognitive network neuroscience | healthy aging

The recollection and retelling of personal past experiences vary across individuals and change over the life span (1, 2). Some people recall the rich spatiotemporal context of a prior experience, while others remember relatively few specific details. Similarly, some individuals recount experiences within a deeper semantic context, while others provide little background information. While not orthogonal, these ways of remembering reflect varying proclivities to access episodic and nonepisodic information during autobiographical recollection. Several factors may influence how individuals remember the past, including age. With advancing age, the episodic quality of memories diminishes as semantic features become more prominent, leaving recollections with increasing amounts of nonepisodic information (2).

Neuropsychological studies have identified the hippocampus and temporal pole (TP) as necessary for episodic and semantic aspects of autobiographical memory (AM), respectively (e.g., refs. 3–5). Task activation studies have found AM to involve a more distributed set of brain regions within the default network (DN) (6–9). The hippocampus and TP may, therefore, coordinate the retrieval of different memory representations with regions of the DN for coherent autobiographical recall (10–12). However, little is known about how the hippocampus and TP specifically interact with the DN and whether these interactions relate to individual differences in AM recollective styles.

The DN can be divided into a core set of regions and two subnetworks, each of which loosely maps onto the anterior temporal and posterior medial cortical systems that support different forms of memory-guided behavior (13, 14) (Fig. 1, 3). The dorsal medial DN, corresponding to the anterior temporal system, is made up of regions functionally affiliated with the dorsomedial prefrontal cortex (dmPFC), including the TP (13). This subnetwork is implicated in semantic-like tasks, such as abstract processing, mentalizing, and language comprehension (15). The medial temporal DN, corresponding to the posterior

Significance

Autobiographical memory includes the recollection of both episodic and semantic content, which has been shown to engage the default network. The present study examines how regions associated with the coordinated retrieval of different types of details are intrinsically connected to the default network and how these connectivity patterns in turn relate to autobiographical recall in younger and older adults. Connectivity within this circuit scaled with the tendency to recall one's personal past with a balance of episodic and semantic detail. Young adults showed a distinct signature of connectivity related to more detailed recollection overall. Our findings provide a high-resolution map of connectivity within the default network and evidence for how variation in this map is sensitive to individual differences in autobiographical recollection.

Author contributions: R.S., G.R.T., and R.N.S. designed research; R.S. performed research; L.M.-T. contributed new reagents/analytic tools; R.S. analyzed data; R.S., L.M.-T., S.S., G.R.T., and R.N.S. edited the paper; and R.S., S.S., G.R.T., and R.N.S. wrote the paper.

The authors declare no competing interest.

This article is a PNAS Direct Submission.

Copyright © 2022 the Author(s). Published by PNAS. This article is distributed under [Creative Commons Attribution-NonCommercial-NoDerivatives License 4.0 \(CC BY-NC-ND\)](https://creativecommons.org/licenses/by-nc-nd/4.0/).

¹To whom correspondence may be addressed. Email: rsetton@fas.harvard.edu or nathan.spreng@gmail.com.

This article contains supporting information online at <http://www.pnas.org/lookup/suppl/doi:10.1073/pnas.2203039119/-/DCSupplemental>

Published October 3, 2022.

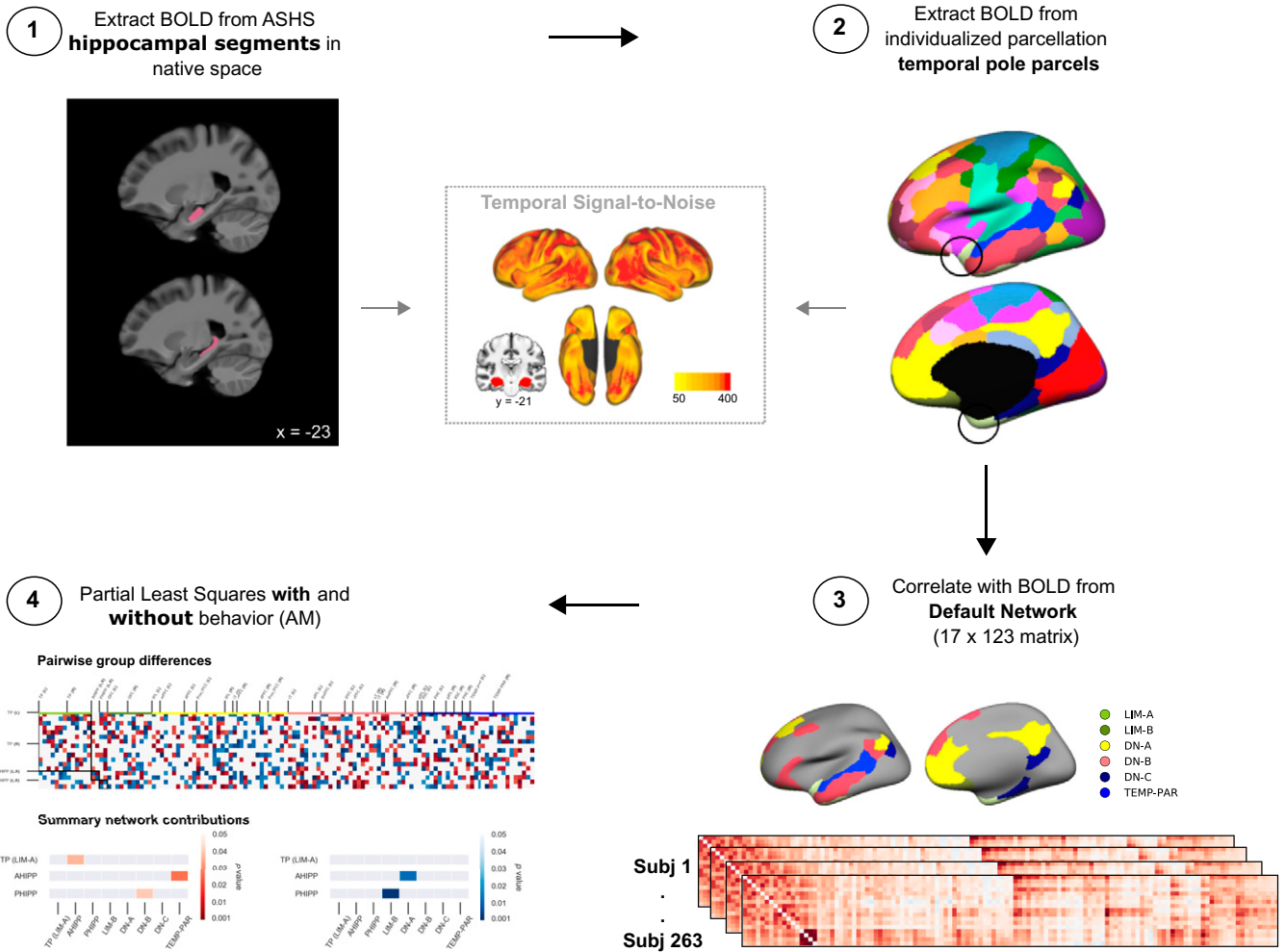


Fig. 1. Schematic of the analytical workflow. (1) BOLD data were extracted from left and right AHIPP and PHIPP segments, as output from ASHS. (2) BOLD data were extracted from TP parcels as defined by each participant's individual-specific parcellation solution. *Inset* shows the temporal signal-to-noise map thresholded to 50 to 400 for visualization purposes. The group temporal signal-to-noise ratio map was masked with the right and left hippocampus probability maps using the Harvard-Oxford Subcortical Structural Atlas in FSL for display only. Temporal signal-to-noise values were sufficiently high to examine RSFC within all regions included in the present analyses (*SI Appendix, Fig. S1*). (3) Functional connectivity between the TP, AHIPP, and PHIPP parcels and LIM, DN, and TEMP-PAR subnetwork parcels were constructed for each participant, resulting in a 17×123 rectangular matrix. (4) Matrices were submitted to PLS to examine patterns of maximal covariance with group assignment or AM density scores from the Autobiographical Interview. The resultant matrix of regional pairwise connections was summarized by network contribution plots illustrating the most reliable within- and between-network connections. See Table 1 for subnetwork and region abbreviations.

medial system, comprises regions functionally affiliated with the medial temporal lobe, including the hippocampus (13). This subnetwork is associated with more episodic simulation abilities, such as AM, future thinking, scene construction, and situating items within a spatial context (15, 16). The precise functional architectures of the hippocampus and TP within and between these discrete network ensembles are not well characterized. It also remains to be determined whether variability within these ensembles scales with variability in AM across individuals.

An age-related shift in the quality of AM recollection coincides with robust changes to the functional integrity of the DN. Specifically, connectivity within the DN is reduced in older adults and more integrated with other large-scale networks (17). Compared with younger adults, older adults show reductions within core regions and the dorsal medial subnetwork but relative preservation of connectivity within the medial temporal subnetwork (18). An open question is whether the shift to semantic-laden AMs in older age is related to functional reorganization of the DN. Here, we determine whether individual differences and age effects in one's tendency to recall more

detailed AMs are related to the integrity of the functional ensembles that comprise the DN.

Our approach was to examine how hippocampus and TP resting-state functional connectivity (RSFC) with the DN covaries with individual differences in AM. RSFC reflects a combination of genetic and experience-dependent changes to functional interactions (19). Individual differences in these functional dynamics may map onto individual differences in behavior, including the propensity to retrieve certain details when describing past experiences. Indeed, self-reported appraisal of recalling one's personal past with more episodic detail has been associated with RSFC between the medial temporal lobes and posterior visual regions, a pattern similar to functional connectivity during visual episodic memory tasks (20, 21). Self-reported semantic-based remembering has been associated with medial temporal lobe RSFC to the prefrontal cortex (PFC) (20). Initial evidence from a small sample of older adults suggests that RSFC of the medial temporal lobe may relate to objective AM performance (22). A distinction between ensembles in a well-powered sample of younger and older adults has yet to be reported.

Table 1. Regions of an extended DN and subnetwork affiliations

| Subnetwork | Regions |
|--|---|
| AHIPP | Left and right anterior hippocampus (AHIPP) |
| PHIPP | Left and right posterior hippocampus (PHIPP) |
| Limbic Network A (LIM-A) | Left and right temporal pole (TP) |
| Limbic Network B (LIM-B) | Left and right orbitofrontal cortex (OFC) |
| Default Network A (DN-A; core regions) | Left and right inferior parietal lobule (IPL), dorsal prefrontal cortex (dPFC), medial prefrontal cortex (mPFC), precuneus and posterior cingulate cortex (Prec/PCC), and right inferior temporal cortex (IT) |
| Default Network B (DN-B; dorsal medial subnetwork) | Left and right lateral temporal cortex (IT), anterior temporal cortex (aT), anterior inferior parietal lobule (aiPL), dorsal medial prefrontal cortex (dmPFC), lateral prefrontal cortex (lPFC), and ventral prefrontal cortex (vPFC) |
| Default Network C (DN-C; medial temporal subnetwork) | Left and right posterior inferior parietal lobule (piPL), retrosplenial cortex (RSC), and parahippocampal cortex (PHC) |
| Temporoparietal Network (TEMP-PAR) | Left and right temporoparietal cortex |

Subnetwork is used to refer to bilateral hippocampal regions as well as subnetworks from the Yeo 17-network solution (32).

We first characterized anterior hippocampus (AHIPP), posterior hippocampus (PHIPP), and TP RSFC with an extended DN (Table 1 shows affiliations and abbreviations) in healthy younger and older adults. The hippocampus was segmented along its longitudinal axis to inspect whether anterior and posterior regions showed differential RSFC patterns with regions throughout the DN (23). Second, we applied multivariate partial least squares (PLS) to test for age group differences in RSFC. We predicted that younger adults would show more differentiated DN subnetworks than older adults, reflected in stronger RSFC between the TP and the dorsal medial subnetwork and between the hippocampus and the medial temporal subnetwork. Finally, we used behavioral PLS to examine how these RSFC profiles related to individual differences in AM and whether these associations differed between younger and older adults. We predicted that episodic AM would associate with RSFC between regions of the hippocampus and the medial temporal subnetwork. Conversely, we predicted that semantic AM would relate to TP RSFC with the dorsal medial subnetwork. Evidence for this dissociation across all participants would fit into a broader framework of separable distributed network ensembles (or “process-specific assemblies”) (24), discernible at rest, configured to support different dimensions of AM (14, 25). We also hypothesized that RSFC associations with AM may differ by age group, reasoning that RSFC differences may underlie the age-related shift in episodic detail generation. The overarching goal was to link RSFC of temporal lobe structures integral for AM to variability in AM performance across individuals.

Results

In the largest sample of AM and RSFC reported to date, we examined hippocampus and TP RSFC with the DN and its relationship to AM (Fig. 1). We collected multiecho (ME) resting-state fMRI from a cohort of healthy younger and older adults and applied individualized cortical parcellations to test network and region-specific connectivity patterns. These innovations boost fMRI signal-to-noise ratios (26, 27) (*SI Appendix, Fig. S1*), reduce age confounds associated with spatial normalization to a standard template (28), and account for individual variability in DN subnetworks (e.g., ref. 29). We implemented a hippocampal segmentation protocol optimized for use in older adult brains to investigate the separable contributions of AHIPP and PHIPP to AM (12, 24, 30) while accounting for age-related variability in this region. Finally, the autobiographical interview (2, 31) was administered as a gold standard measure of episodic (internal) and semantic (external) AM. Combined, these steps enhanced our power to detect how RSFC of AHIPP, PHIPP, and TP with the DN (Table 1) associated with individual differences in AM. Our analysis proceeded in three steps: characterizing RSFC of the circuit, testing for age group differences, and identifying associations with internal and external AM as a function of age group. At each turn, regional effects are summarized by network effects, reflecting the most reliable within- and between-network connections (Fig. 1, 4 and *Materials and Methods*).

RSFC of AHIPP, PHIPP, and TP with the DN. We first established how AHIPP, PHIPP, and TP were functionally connected with regions across the extended DN. We define the extended DN as regions from the default, limbic (LIM), and temporoparietal (TEMP-PAR) subnetworks from the Yeo et al. (32) 17-network solution. A surface representation of the AHIPP, PHIPP, and TP RSFC pattern across all participants is shown in Fig. 2*A*. TP showed strong positive connections with itself and lateral temporal cortex (IT). AHIPP and PHIPP showed strong positive midline connections to anterior and posterior structures, respectively. Weak negative connections were also observed between AHIPP/PHIPP and ventral prefrontal cortex (vPFC).

Average matrices show RSFC of AHIPP, PHIPP, and TP by hemisphere in younger and older adults separately (Fig. 2*B*). Regions are organized and color coded by their subnetwork affiliations from Yeo et al. (32) (Table 1). Notably, yellow corresponds to regions within the DN core (DN-A), coral corresponds to regions within the dorsal medial DN (DN-B), and navy corresponds to regions within the medial temporal DN (DN-C). Blue corresponds to TEMP-PAR regions, which are affiliated with the DN at coarser resolutions (32) and are consistent with other parcellation characterizations of a language network (33).

RSFC patterns were similar across groups. All three regions of interest showed broad correspondence to their DN subnetworks; TP showed a strong positive connection to lateral temporal regions within DN-B and TEMP-PAR, and AHIPP/PHIPP showed positive connection to midline regions, including orbitofrontal cortex (OFC) and medial prefrontal cortex (mPFC), as well as regions within DN-C. Of these, ipsilateral connections were often stronger than contralateral. *SI Appendix, Fig. S5A* reproduces these matrices, highlighting negative connections in younger adults that were nonsignificant or positive in older adults.

Age Group Differences in RSFC. Quantitative comparison of the 2,091 pairwise connections revealed a pattern of connectivity that distinguished younger and older adult RSFC (permuted

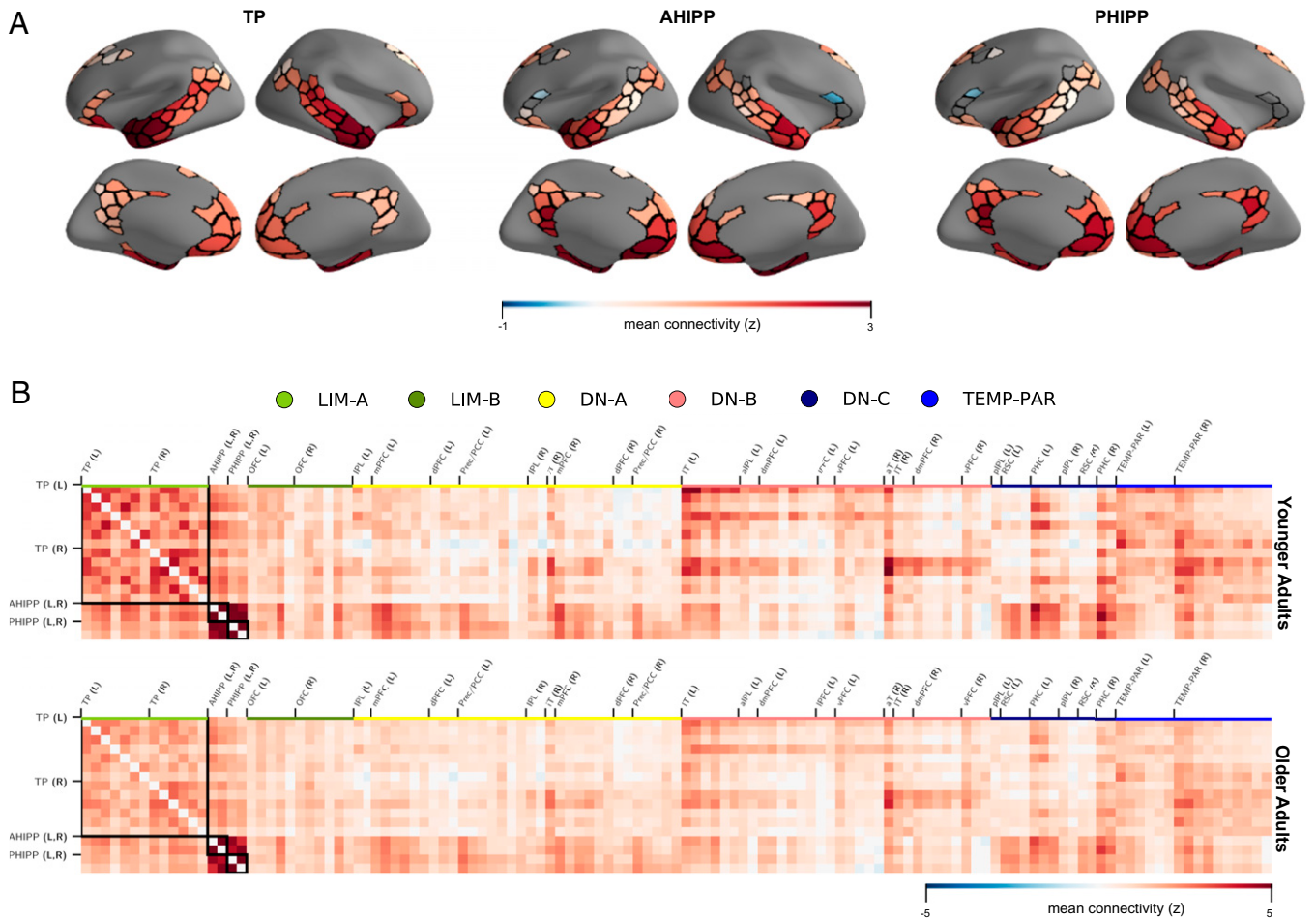


Fig. 2. RSFC of AHIPP, PHIPP, and TP with the DN. (A) RSFC for each region of interest across the extended DN collapsed across younger and older adults. For each region, BOLD data were averaged across parcels from both hemispheres to construct a new 1×109 RSFC matrix. z values were averaged across all participants. The significance of each cell was determined with a one-sample t test. P values below 0.05 were masked out. Hippocampal regions are not shown on the surface. For visualization purposes, all TP parcels on the TP surface were assigned the maximum value in the matrix to indicate self-connection. (B) Average RSFC in younger (Upper) and older (Lower) adults shown in full. Bootstrap resampling (resampling rate = 10,000) was implemented to obtain a 95% CI and determine reliable connections. Connections whose CIs crossed zero were masked out. Regions of the extended DN (presented horizontally across the matrices) are organized and color coded by subnetwork affiliation according to the Yeo et al. (32) 17-network solution. See Table 1 for region abbreviations. L, left; R, right.

$P < 0.001$) (Fig. 3 A–C). Network contribution analyses summarize the significant contributions of within- and between-network edges to this pattern (Fig. 3B). Significant regional connectivity differences are discussed in the context of network-level effects.

Younger adults showed greater connectivity within TP, AHIPP, and PHIPP, reflected in connections across hemispheres within each region. Younger adults expressed stronger connectivity than older adults along the longitudinal axis of the hippocampus, showing both ipsilateral and contralateral connections between AHIPP and PHIPP. Intra-TP and TP connectivity with AHIPP and PHIPP were reliably greater in younger compared with older adults at the network level. At the regional level, younger adult TP connectivity was also greater with regions throughout DN-B and TEMP-PAR in both hemispheres, including IT, anterior inferior parietal lobule (aIPL), dmPFC, vPFC, and most regions of the TEMP-PAR cortex. In younger adults, select anterior medial TP parcels showed greater preferential connection to bilateral regions throughout DN-A and DN-C, including mPFC, dorsal prefrontal cortex (dPFC), parahippocampal cortex (PHC), and posterior inferior parietal lobule (pIPL). Greater bilateral AHIPP connections were also observed with these anterior medial TP parcels in younger adults. Greater AHIPP–DN-C network connections in younger adults were reflected in bilateral AHIPP

connectivity to PHC and right pIPL. PHC, as part of DN-C, is more often associated with PHIPP as part of a posterior medial temporal lobe pathway (23). Greater PHIPP connectivity to PHC was also observed but to a lesser extent. Greater PHIPP–OFC connections reliably contributed to the overall network pattern, although AHIPP–OFC connections were also observed with more medial and rostral OFC parcels.

Older adults had a distinct pattern of greater between-network RSFC, which in part, reflected reduced anticorrelation (SI Appendix, Fig. S5B), compared with younger adults. The first of these was greater TP connectivity, marked by TP–DN-A and TP–DN-C at the network level. At the regional level, this result emerged as bilateral TP connectivity with precuneus (Prec)/posterior cingulate cortex (PCC), right dPFC, and retrosplenial cortex (RSC). These regional connections were notably less negative and even positive in older adults (SI Appendix, Fig. S5B). The most reliable AHIPP RSFC differences in older compared with younger adults were with prefrontal DN-B regions, including dmPFC and lateral prefrontal cortex (lPFC). Similar connections were observed with PHIPP. Greater AHIPP and PHIPP connectivity was also observed with left Prec/PCC. Overall, older adults showed greater hippocampal connectivity across regions within DN-A and DN-B, whereas younger adults had stronger

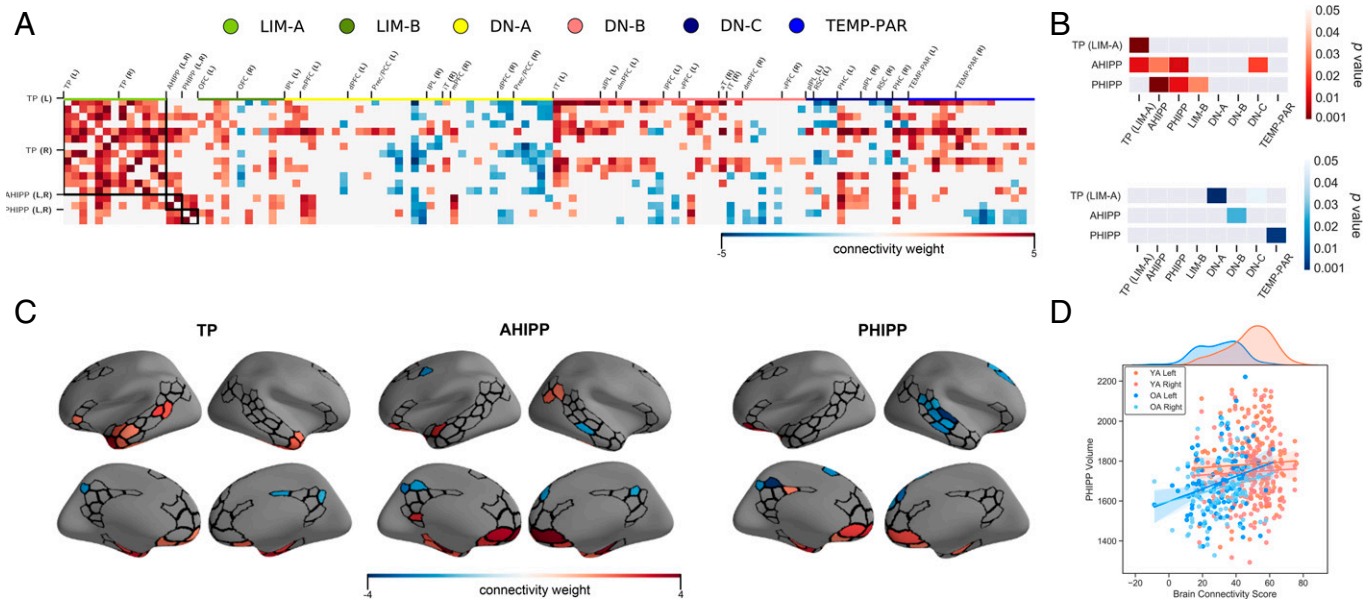


Fig. 3. Age group differences in RSFC. (A) One pattern distinguished pairwise connectivity expressed more by younger adults, shown in warmer colors, from pairwise connectivity expressed more by older adults, shown in cooler colors. The matrix was thresholded at a bootstrap ratio of 1.96, representative of a 95% CI. Regions of the extended DN (presented horizontally across the matrix) are organized and color coded by subnetwork affiliation according to the Yeo et al. (32) 17-network solution. See Table 1 for region abbreviations. (B) Network contributions summarizing network-level differences. (C) A surface representation of A. For each region of interest, unthresholded results were averaged across parcels in the left and right hemispheres and then, thresholded to an average bootstrap ratio of 1.96. Hippocampal regions are not shown on the surface. (D) Brain connectivity scores from A plotted as a function of PHIPP volume in younger and older adults. In older adults, higher brain connectivity scores were related to larger bilateral PHIPP volumes. L, left; R, right; YA, younger adults; OA, older adults.

hippocampal connections with DN-C regions. Hippocampus may, therefore, bind the posterior cortex to the DN in younger age (e.g., ref. 34) but not into older adulthood. Indeed, older adults showed a striking pattern of greater PHIPP–TEMP-PAR connectivity emerging from bilateral PHIPP connections to the right TEMP-PAR cortex.

We next tested whether this pattern was influenced by gray matter volumes of the three regions of interest. As seen in Fig. 3D, larger PHIPP volumes in the left hemisphere (and marginally in the right) were associated with higher brain connectivity scores in older adults only (left: $p(99) = 0.25$, $P < 0.05$, $[0.06, 0.42]$; right: $p(99) = 0.18$, $P = 0.06$, $[-0.01, 0.36]$). Older adults with larger PHIPP volumes had a pattern of RSFC more similar to that expressed by younger adults. This relationship was statistically attenuated when site was included as a covariate (SI Appendix, Fig. S3 and Tables S3 and S4). AHIPP and TP volumes were not related to RSFC (all P values were >0.05).

RSFC Associations with AM. AM was tested with the Autobiographical Interview (2). As part of the interview, participants chose a single memory, specific in time and place, to describe in detail for a series of different time periods (e.g., childhood, teenage years, etc.). Descriptions were scored for episodic-like “internal” details (i.e., order of events, location, time information, sensory descriptions, emotions, thoughts) and semantic-like “external” details (i.e., general semantic information about oneself and the world, repetitions, metacognitive statements, specific details about unrelated memories). A full subcategory listing is detailed in SI Appendix, Table S5 and S6. The number of internal and external details is typically tallied and averaged across events. Work from our laboratory has shown that measures controlling for verbosity, which we refer to as internal and external density scores, are more reliable and valid metrics of AM (31).

We have previously examined how internal and external density scores in this sample were associated with gray matter volumes of AHIPP, PHIPP, and TP (35). We reported that older adults had

less internally dense and more externally dense recollections than younger adults (internal density: $M_{\text{young}}: 0.09$, $SD_{\text{young}}: 0.02$, $M_{\text{old}}: 0.07$, $SD_{\text{old}}: 0.02$, $t(258) = 11.06$, $P < 0.001$, Cohen’s $d = 1.38$; external density: $M_{\text{young}}: 0.02$, $SD_{\text{young}}: 0.01$, $M_{\text{old}}: 0.04$, $SD_{\text{old}}: 0.01$, $t(258) = 6.32$, $P < 0.001$, Cohen’s $d = 0.79$).

Here, we tested for RSFC patterns associated with internal and external density scores. To do so, we used behavior PLS to identify patterns of RSFC in younger and older adults that covaried with internal and external density scores. PLS was carried out in the same 2,091 pairwise connections between our three regions of interest—AHIPP, PHIPP, and TP—and regions of the extended DN. Two significant latent variables emerged.

An age-invariant pattern of RSFC dissociates internal from external density.

The first pattern revealed a main effect of detail density, separating RSFC associated with internal vs. external density in both younger and older adults (18.77% covariance explained, permuted $P < 0.001$) (Fig. 4A). In both age groups, greater internal density of AM recollection was associated with higher RSFC between a number of regions (Fig. 4A, warmer colors). First, internal density was positively associated with greater TP–LIM-B, AHIPP–LIM-B, and bilateral PHIPP RSFC. At the regional level, left-lateralized TP connections were observed with regions throughout the extended DN. Right TP connections were observed with mPFC regions, including OFC, mPFC, and dmPFC, as well as TEMP-PAR cortex. Bilateral AHIPP connections to OFC were most reliable, although AHIPP connections across hemispheres and to right mPFC were also observed. Internal density was also associated with RSFC between right PHIPP and PHC.

In both younger and older adults, greater external density was related to higher TP–TEMP-PAR connectivity. This included contralateral connections between TP and TEMP-PAR cortex. Contralateral connections were also observed between right TP and left DN-B regions, including IT, IPFC, and vPFC in association with greater external density.

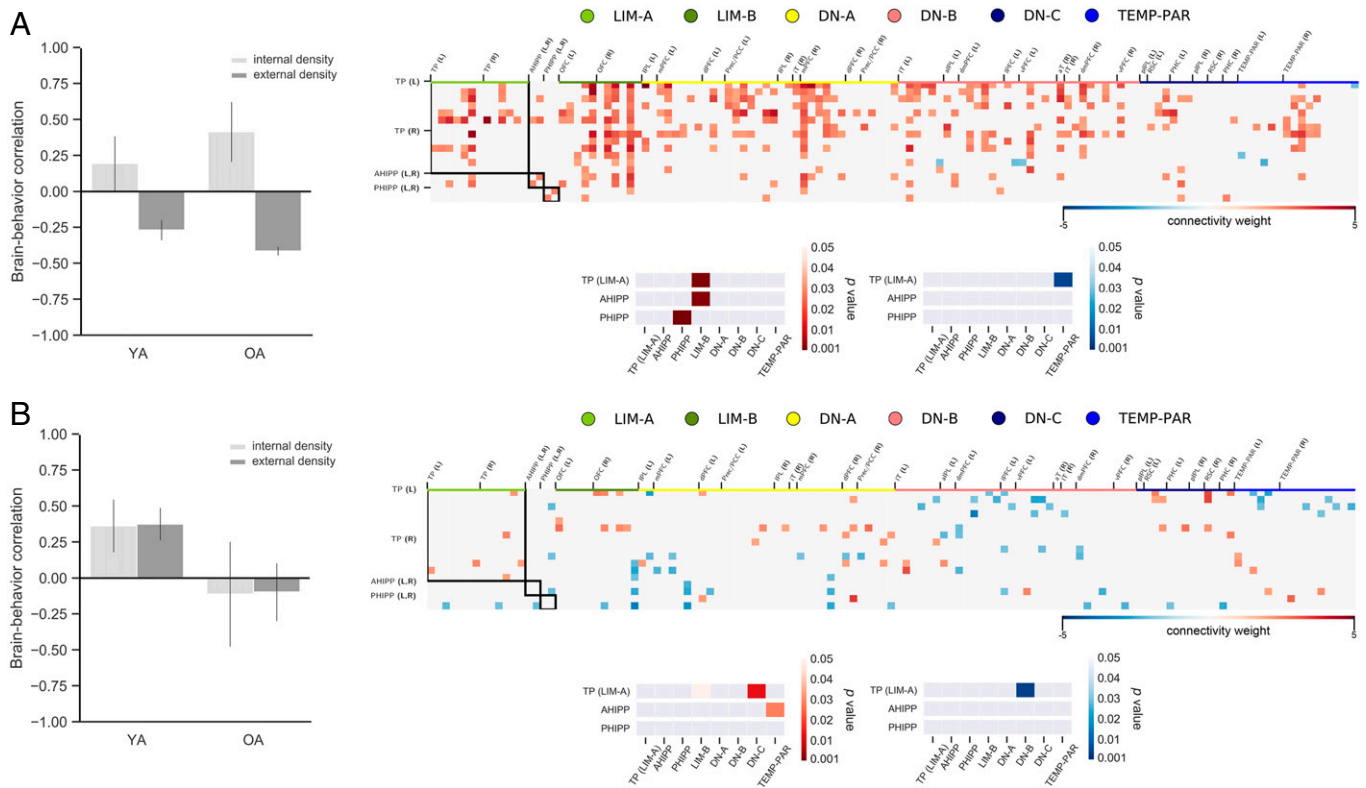


Fig. 4. Individual differences in internal and external density related to RSFC. Two significant patterns of functional connectivity associated with internal and external density as a function of age group were identified by behavior PLS analysis. (A) A main effect of detail density distinguished pairwise connections related to internal (warmer colors) and external (cooler colors) density in both younger adults and older adults. (B) A main effect of age group shows pairwise connections associated with both internal and external density in younger adults. Warmer colors reflect pairwise connections positively associated with density scores while cooler colors reflect pairwise connections negatively associated with density scores. Network contribution plots characterize network-level effects. Regions of the extended DN (presented horizontally across the matrices) are organized and color coded by subnetwork affiliation according to the Yeo et al. (32) 17-network solution. See Table 1 for region abbreviations. L, left; R, right; YA, younger adults; OA, older adults.

RSFC associations with density scores were highly similar when controlling for sex, education, estimated whole-brain volume (eWBV), and framewise displacement. Including site as an additional covariate attenuated external density associations in younger adults (*SI Appendix, Fig. S4 and Tables S5 and S6*).

We next conducted a post hoc analysis to explore which subcategories of internal and external details most contributed to the RSFC–density associations within each age group. RSFC associations with internal density were driven by internal event details in younger adults and internal event, time, perceptual, and emotion/thought details in older adults (*SI Appendix, Table S5*). RSFC associations with external density were driven by external place, perceptual, semantic, repetition, and other details in younger adults and external event, place, time, perceptual, and emotion/thought details in older adults. Sex, education, framewise displacement, and eWBV were included as covariates. Including site as an additional covariate reduced the magnitude of RSFC associations with external density, but results remained qualitatively similar (*SI Appendix, Table S6*).

A specific pattern of RSFC in younger adults for internal and external density. The second significant pattern was observed in younger adults, where internal and external density covaried together (1.97% covariance explained, permuted $P < 0.05$) (Fig. 4B). Internal and external density scores in younger adults were both positively associated with TP–LIM-B, TP–DN-C, and AHIPP–TEMP-PAR connections at the network level (Fig. 4B, warmer colors). Regionally, left TP showed both ipsi- and contralateral connections to OFC, RSC, and PHC. Left AHIPP was connected to TEMP-PAR cortex both ipsi- and

contralaterally, while right AHIPP connectivity to TEMP-PAR cortex remained ipsilateral. AM in younger adults was thus associated with left intra- and interhemispheric RSFC within an extended DN. Internal and external density scores in younger adults were negatively associated with TP connectivity to DN-B. Specifically, younger adult AM was associated with less connectivity between left-lateralized TP connectivity to aIPL, dmPFC, lPFC, and vPFC (Fig. 4B, cooler colors). Notably, internal and external density scores in younger adults were also negatively associated with AHIPP and PHIPP connectivity to anterior midline regions, including OFC and mPFC, as well as with right PHIPP connectivity throughout the extended DN. RSFC associations with density scores were nearly identical when controlling for sex, education, framewise displacement, eWBV, and site.

Post hoc associations with detail subcategories were again conducted to determine which details contributed to the shared density association with RSFC in younger adults. Internal event, place, and time details along with external event, place, time, perceptual, emotion/thought, and other details drove the RSFC–density association (*SI Appendix, Table S5*). When site was included as a covariate, RSFC associations with internal detail categories were nearly identical. Only external event and emotion/thought detail categories significantly contributed to the pattern (*SI Appendix, Table S6*).

Discussion

Our findings provide a high-resolution map of RSFC between temporal lobe structures and regions throughout the DN, as

well as differences with age. They also provide evidence that RSFC of AHIPP, PHIPP, and TP with the DN is related to individual differences in autobiographical recollection. We first established the RSFC profiles of key regions involved in AM and tested for differences between younger and older adults. Across participants, TP was strongly connected to lateral temporal regions. AHIPP and PHIPP were strongly connected to regions of the medial temporal DN subnetwork, including OFC. Compared with older adults, younger adults had greater RSFC between both hippocampal regions and OFC. As predicted, older adults had lower RSFC within AHIPP, PHIPP, and TP but greater RSFC between AHIPP, PHIPP and TP with distributed regions of the DN. This pattern of higher and lower RSFC was associated with PHIPP volumes in older adults, suggestive of a link between local structural and distributed functional differences with age. When RSFC was related to individual differences in AM, a common pattern emerged across age groups. Internal density was associated with greater AHIPP and TP connectivity to OFC and intra-PHIPP connectivity. External density was associated with higher TP connectivity to regions across the IT and TEMP-PAR cortex. Younger adults also demonstrated a unique pattern of AM related to RSFC; the tendency to recall a higher density of autobiographical detail was associated with greater TP connectivity to OFC and RSC, greater AHIPP connectivity to TEMP-PAR cortex, and lower TP connectivity to PFC. Our findings reveal that individual differences in RSFC of key temporal lobe structures with the DN explain individual differences in AM recollective styles.

Age Group Differences in RSFC of AHIPP, PHIPP, and TP. A multivariate comparison of RSFC between age groups revealed that older adults had less connectivity within TP, AHIPP, and PHIPP as well as less connectivity between AHIPP and PHIPP, largely consistent with prior work (36–38). This pattern recapitulates a pattern of large-scale network dedifferentiation across the healthy aging connectome (28, 39, 40). Reduced connectivity within AHIPP and within PHIPP suggests a nonspecific reduction in functional connectivity across the hippocampal longitudinal axis in older adults.

TP showed greater affiliation with lateral temporal regions in younger adults, corresponding to a dorsal medial DN subnetwork (41) (Fig. 1, 3, coral colors). Younger adults also had greater TP RSFC with TEMP-PAR regions. The TEMP-PAR network, as defined by the Schaefer atlas (42), includes frontal and temporal parcels specialized for language processing (33). Increasing evidence suggests that a purported language network may be distinct from but spatially adjacent to other default subnetworks (43, 44). The TP has been robustly implicated in language processing (e.g., ref. 45), and greater TP RSFC to TEMP-PAR cortex in younger adults may correspond to a more robust language network in both hemispheres.

Our analysis also revealed heterogeneity in TP RSFC in younger adults. Select anterior medial portions of TP were connected to core DN regions and PHC. AHIPP connectivity to this same TP region was among the most reliable connections in younger adults, along with AHIPP connectivity to PHC. Indeed, anterior medial TP may be more cytoarchitecturally similar to medial TP, which is homologous to ventral TP in nonhuman primates (46). Stronger RSFC of this TP region may be expected along the medial extent of the temporal lobe, such as with PHC, and may hence show similarities to PHC RSFC (47). Given its proximity and connection to AHIPP, this anterior medial TP region may be uniquely located to pivot between DN subnetworks. In older adults, TP was less

functionally associated with dorsal medial DN regions, instead correlating more—and less selectively—with posterior core and medial temporal DN regions, connections that were notably negative in younger adults. This converges with prior evidence of dedifferentiation in the dorsal medial DN subnetwork (18) and reduced anticorrelation of regions within the medial temporal lobe and posterior DN in older adults (34). The more widespread connectivity between TP and posterior DN regions may also suggest decreased functional heterogeneity within the TP in older adulthood.

AHIPP and PHIPP RSFC in younger adults revealed a tighter correspondence to the medial temporal DN subnetwork than older adults, as evidenced by greater RSFC to PHC, mPFC, and OFC (41) (Fig. 1, 3, navy colors). This finding diverged from prior work identifying PHC as preferentially connected to PHIPP as part of a posterior medial network (14, 23). In older adults, greater hippocampal RSFC was most prominently observed between PHIPP and the TEMP-PAR cortex. In fact, older adults had greater RSFC for both AHIPP and PHIPP with distributed regions throughout the DN. This was in contrast to work finding lower RSFC between PHIPP and core regions of the DN alongside increased connectivity within PHIPP in older adults (36–38). These inconsistencies may be due to differences in analysis choices, including the extent of regions tested for RSFC differences, functional boundary mapping (e.g., hippocampal body as PHIPP instead of AHIPP) (48), smaller samples sizes, and poorer temporal signal-to-noise ratios. The present work overcomes many of these methodological challenges to characterize age differences in RSFC throughout the DN. The combination of techniques applied here—ME fMRI for improved signal detection (*SI Appendix*, Fig. S1), hippocampal segmentation with an atlas optimized for use in older adults, and individualized parcellation for individual-specific demarcation of functional regions—provides unprecedented precision in characterizing this network.

RSFC differences across groups were related to PHIPP gray matter volume. We recently reported that older adults have smaller PHIPP gray matter volumes compared with younger adults, with no differences observed in AHIPP or TP (35). Here, larger PHIPP volumes in older adults were related to stronger expression of the “young-like” RSFC pattern. This finding suggests a link between local structural and distributed functional differences in older compared with younger adults (49). We speculate that the observed age differences in RSFC may be driven by gray matter atrophy to the PHIPP. Including site as a covariate attenuated this relationship, yet controlling for site removes desirable demographic variability that may have even more pronounced effects on older adult brain structure and function (e.g., ref. 50) (*SI Appendix*). Replication in larger, diverse samples will be necessary to advance our understanding of age differences in structure–function relationships within the temporal lobe, particularly where longitudinal data are lacking.

An Age-Invariant Pattern of RSFC Dissociates Internal from External Autobiographical Recollection. Despite age differences in the functional architecture of the AM circuit under examination, individual differences in internal and external AM were dissociated in their patterns of RSFC across the full sample. This is consistent with task-related findings showing that younger and older adults engage similar regions during AM (51–53), although older adults demonstrate more robust bilateral activation of medial and lateral temporal lobe regions (54). Task studies have also identified activity that differs between younger and older adults (51). These differences are often

attributed to the reduced episodic content of recollection in older age, although few studies have explicitly linked task activation to individual differences in AM. The advantage of the approach used here is that RSFC dissociated internal and external AM, providing evidence for separable distributed network ensembles that may be configured to support different aspects of AM (14, 25). Similar approaches have been used to identify such ensembles in association with self-reported AM abilities (e.g., ref. 20). We extend these findings to objective AM performance and suggest that RSFC differences may offer insight into why individuals vary in how they recount the past.

Individuals with more internally dense recollections had greater RSFC between AHIPP/TP and OFC and within PHIPP. AHIPP, TP, and OFC are anatomically and functionally connected as part of the dorsal medial DN. Together, these regions are predicted to play a role in familiarity-based recognition, social and emotional processing, and semantic knowledge representation (14, 23, 55). Our results suggest that variation in RSFC among these regions may also scale with episodic processes. While self-reported episodic AM abilities in younger adults have been associated with RSFC between the hippocampus and posterior medial regions (20, 21), a more distributed set of regions active during AM has been related to subjective ratings of imagined detail in younger and older adults (51). We expand on this with evidence for how the magnitude of connectivity among AHIPP, PHIPP, and TP relates specifically to a performance-based measure of episodic AM.

RSFC between AHIPP/TP and OFC systematically increases through adolescence concurrent with the development of complex cognitive functions (56, 57). RSFC between these regions in association with internal AM may reflect fluid aspects of everyday remembering. AHIPP is thought to support recollection of coarse or more generalized AM information, as would be expected in early stages of memory construction prompted by open-ended retrieval cues (12). Effective connectivity models have demonstrated interactions between AHIPP and fronto-temporal regions during early AM retrieval that precede PHIPP interactions with posteromedial regions during later elaboration (58). Activity in ventromedial PFC, which spans OFC, is associated with temporarily binding schema representations from across the cortex to form higher-order knowledge templates (59). When certain schemas are activated, ventromedial PFC can then bias information processing in a context-sensitive manner. Studies leveraging the higher temporal resolution of magnetoencephalography during AM have shown that ventromedial PFC activity during construction drives hippocampal activity that is then sustained throughout elaboration (60). TP is often associated with semantic processes and incorporating prior knowledge into encoded representations (e.g., refs. 61 and 62). Functional interactions among AHIPP, TP, and OFC could putatively reflect context-dependent retrieval that takes place in OFC; representations of associated episodes in AHIPP arrive at OFC and activate specific schemas that then call on relevant prior knowledge from TP, all to engage and retrieve context-appropriate representations from PHIPP. The observed pattern of greater RSFC for more internally dense AMs may, therefore, reflect connections forged as a result of repeated efficient context-dependent retrieval. This pattern of RSFC may be weaker with a reduced capacity for context-dependent retrieval and internal episodic AM.

The predominance of left TP connections associated with internal AM suggests a link to language. Although TP has been associated with the dorsal medial DN subnetwork (13), which plays a role in semantic processing (15), it has also shown strong affiliation to a left-lateralized language network (e.g., ref. 43).

Language is inextricably linked to autobiographical recollection, which may explain why episodic AM more often engages regions in the left hemisphere (6). The extent to which semantic processes that support memory overlap with semantic processes that involve language—and the role TP may play in each—remains to be determined. Left TP RSFC related to higher internal density was observed with TEMP-PAR regions belonging to the language network but more so with regions throughout the DN. TP may be particularly well suited to flexibly couple between regions that support both language and memory processes.

Our findings relate TP RSFC with lateral temporal and prefrontal regions to a greater propensity for external AM across individuals. A stronger association in older adults further suggests a shift toward relying more on external information when recalling personal memories in older age. IT, IPFC, and TEMP-PAR cortex are all predicted to communicate bidirectionally with anterior temporal regions, including the TP, during semantic cognition (61). The observed interregional connections related to external AM underscore that variation in RSFC across these specific regions is sensitive to variation in external AM. Although we did not have predictions about the laterality of effects, external AM was exclusively associated with contralateral TP connectivity. When examining the subcategory contributions to this RSFC pattern, we found that external semantic details contributed most to the association in younger adults, while external event, place, time, perceptual, and emotion/thought details contributed most in older adults (*SI Appendix, Tables S5 and S6*). In other words, younger adults showed separable RSFC associations between episodic and semantic details, whereas older adults showed separable RSFC associations between relevant and irrelevant episodic information. It is possible that RSFC related to semantic information in older adults is less distinguishable from that of relevant episodic information if, with age, episodic detail is “semanticized,” whereby specific memories gradually lose their spatiotemporal context over time (63). The distinction between relevant and irrelevant episodic details in older adults is especially intriguing given age-related impairments to attention, stemming from a reduced ability to suppress irrelevant information (e.g., ref. 64). AM studies tend to center on the internal, episodic quality of recalling the past, yet better characterization of the external aspects of AM, especially in older age, can provide much needed insight into the neurocognitive contributions of shifts in narrative storytelling (65).

An RSFC Pattern Associated with Autobiographical Recollection in Younger Adults.

Younger adults displayed a unique pattern of RSFC associated with AM. In this pattern, internal and external density covaried together, revealing a network ensemble specific to younger adult recollection. More detail-dense recollections were associated with greater RSFC between the left TP (including the anteromedial TP) and OFC, Prec/PCC, RSC, and PHC. Less dense recollections were related to greater left TP RSFC with PFC and TEMP-PAR cortex. TP RSFC patterns may associate with greater overall AM detail since TP binds high-level social and emotional information (66). Subcategory contributions to this pattern included internal and external event details (*SI Appendix, Tables S5 and S6*). Unlike in older adults, relevant and irrelevant episodic details were similarly related to RSFC in younger adults. Leading models of AM posit that access to our repository of memories is hierarchical; specific episodic experiences are embedded within categories of more general events, which are, in turn, subsumed under lifetime periods (67). Retrieval and reconstruction of an appropriate memory involve sifting through

broader organizing categories to gain access to specific contextual details. Additional interactions, such as those between AHIPP and OFC, may be needed early on to adjudicate the relevance of episodic detail. The absence of this shared pattern of covariance in older adults may suggest altered mechanisms of context-dependent retrieval.

Conclusions

The present study is the largest aging investigation into the neural correlates of AM conducted with the Autobiographical Interview. Leveraging multivariate methods, we were able to move beyond inferences made from silent in-scanner AM tasks to separately examine individual differences in internal and external AM. We acknowledge that the brain–behavior associations presented convey an indirect characterization of age differences in brain function supporting AM (refs. 68 and 69 have similar commentary). Task activation studies are an effective means for identifying brain activity engaged during cognition but offer limited information about how activity varies across people. Using RSFC, here we identified specific network ensembles that systematically vary across individuals in predicting internal and external aspects of AM. Interactions within and between these ensembles are key to understanding individual differences in recollection. These findings largely converge with recent work characterizing separable and combined roles of anterior temporal and posterior medial regions in AM and cognition more broadly (e.g., refs. 12, 14, 58, 60, and 70) and provide testable hypotheses for future task fMRI studies (71). Continued advances in neuroimaging methods, such as real-time motion correction for audible in-scanner AM tasks (72), will be instrumental to further understand the different processes that underlie individual differences in AM.

Materials and Methods

Participants. Participants were 263 healthy younger ($n = 158$; 91 female, 67 male; $M_{\text{age}} = 22.59$, $SD_{\text{age}} = 3.33$) and older ($n = 105$; 58 female, 47 male; $M_{\text{age}} = 68.19$, $SD_{\text{age}} = 6.29$) adults from Ithaca, New York, United States and Toronto, Ontario, Canada (SI Appendix, Table S1). We recently reported on this subset of participants to examine the link between AM and structural MRI (35). This subset comprised participants from a larger sample of participants with AM data (31) who also underwent MRI scanning. Briefly, all participants were screened for histories of neurological or psychiatric disorder, depressive symptomology (assessed with the Beck Depression Inventory or the Geriatric Depression Scale) (73, 74), and mild cognitive impairment (using the Mini-Mental State Examination) (75). Written informed consent was obtained from each participant. Study procedures were administered in compliance with the Institutional Review Board at Cornell University and the Research Ethics Board at York University.

AM. AM was assessed with the Autobiographical Interview (2). Participants were asked to choose a memory from each of three (younger adults) or five (older adults) life stages: childhood, teenage years, early adulthood, middle adulthood, and older adulthood. Participants were instructed to only choose memories that were specific in time and place. Starting with the first memory, participants described the memory chosen in as much detail as possible until they reached a natural end (free recall). Participants were then asked if they remembered anything else about the memory (general probe) before moving onto the next life stage. After all memory descriptions, each memory was revisited, and participants were probed with specific questions to cue episodic recollection (specific probe). Participants then rated the memory for vividness, emotional change, significance, and rehearsal of the memory on a five-point Likert scale. Interviews were audio recorded and transcribed.

Interviews were scored according to the original protocol by trained researchers. According to this procedure, scorers identify the main event in each memory

and subdivide the text into internal details—episodic details related to the event—and external details—primarily semantic details that often provide background. Internal details include information about the sequence of events, location, time, perceptual landscape, and the participant's emotions and thoughts. External details include semantic information, repetitions, metacognitive statements, and other details unrelated to the main event. A full listing of subcategories can be found in SI Appendix, Tables S5 and S6. Tallies are then made for each detail type and for the broader internal and external categories. Text from the specific probe was not considered in the present study. All interviews were double scored and reached high interrater reliability (internal: $r(261) = 0.91$, $P < 0.001$; external: $r(261) = 0.82$, $P < 0.001$).

Work from our laboratory has shown that internal and external detail counts, which may serve as coarse approximations for episodic and semantic recollection, are positively associated with each other and overall word count (31). Dependent variables that control for verbosity have high reliability across memories, remove the positive association between internal and external details, and demonstrate convergent validity with other laboratory performance-based memory tasks. Here, we use one such variable, a density score, which separately divides internal and external counts by a memory's overall word count. Internal and external density scores were averaged across memories to serve as stable measures of episodic and semantic recollection. Density scores for subcategories of internal and external details were also calculated.

Neuroimaging. Imaging data were acquired from both sites with similar scan protocols. Images in Ithaca were acquired with a 3T GE750 Discovery series MRI scanner fit with a 32-channel head coil at the Cornell Magnetic Resonance Imaging Facility. Data in Toronto were acquired on a 3T Siemens TimTrio MRI scanner with a 32-channel head coil at the York University Neuroimaging Center. These data are openly available as part of a recent cross-sectional healthy aging data release (76).

T1-weighted volumetric magnetization prepared rapid gradient echo sequences at each site were as follows: on the GE750 Discovery (TR = 2,530 ms; TE = 3.4 ms; 7° flip angle; 1-mm isotropic voxels, 176 slices, 5 min and 25 s) with 2× acceleration with sensitivity encoding and on the Siemens TimTrio (TR = 1,900 ms; TE = 2.52 ms; 9° flip angle; 1-mm isotropic voxels, 192 slices, 4 min and 26 s) with 2× acceleration and generalized autocalibrating partially parallel acquisition encoding at an integrated parallel acquisition technique acceleration factor of two.

Two 10-min runs of eyes-open resting-state functional MRI were collected with an ME EPI sequence containing three echo times (TE): on the GE750 Discovery (TR = 3,000 ms; TE₁ = 13.7 ms, TE₂ = 30 ms, TE₃ = 47 ms; 83° flip angle; matrix size = 72 × 72; field of view = 210 mm; 46 axial slices; 3-mm isotropic voxels; 204 volumes, 2.5× acceleration with sensitivity encoding) and on the Siemens TimTrio (TR = 3,000 ms; TE₁ = 14 ms, TE₂ = 29.96 ms, TE₃ = 45.92 ms; 83° flip angle; matrix size = 64 × 64; field of view = 216 mm; 43 axial slices; 3.4 × 3.4 × 3-mm voxels; 200 volumes, 3× acceleration, generalized autocalibrating partially parallel acquisition encoding).

Image Processing.

Structure. T1-weighted images were submitted to FreeSurfer version 6.0.1 (77, 78) for cortical reconstruction and volumetric segmentation. Values of estimated total intracranial volume (eTIV), gray matter volume, and white matter volume were extracted. eWBV was calculated as (gray matter + white matter)/eTIV and used as a covariate where indicated.

The medial temporal lobe was segmented with Automatic Segmentation of Hippocampal Subfields (ASHS) (79), which employs multiatlas label fusion to automatically delineate subfields in individual participants. ASHS was run with the ASHS-PMCT1 atlas (80) in both younger and older participants. Outputs were visually inspected for gross errors. As our aim was to examine age differences in AHIPP/PHIPP functional connectivity, we extracted regions of interest for anterior (head) and posterior (tail and body) portions of the hippocampus in each hemisphere (four segments total) (Fig. 1). The hippocampal body is sometimes considered separately (48) or as part of the anterior segment (81). We proceeded with the ASHS results, in line with preceding anatomical segmentations (20, 82). Gray matter volumes were also extracted and adjusted for head size (83, 84).

Function. The functional data preprocessing and analysis here have been previously applied to a larger sample and detailed elsewhere (28). We review them in brief below. A schematic of methodological steps is shown in Fig. 1.

T1-weighted images were skull stripped in FSL with the Brain Extraction Tool(85) using default parameters. Skull-stripped anatomical and functional images were then submitted to ME Independent Components Analysis (86, 87) for minimal preprocessing and denoising. Advantages of ME acquisitions include the ability to better approximate T2*, the transverse relaxation in gradient echo imaging, in every voxel, derive a T2* map of the brain, and optimally combine echoes. The TE-dependence model of blood oxygen level dependent (BOLD) signal drives denoising by separating TE-dependent BOLD signal from TE-independent noise. Together, these provide a significant boost to BOLD signal detection, particularly in regions prone to signal dropout, such as TP and OFC (Fig. 1, *Inset*). Denoised time series were quality checked to flag participants with unsuccessful coregistration, residual noise (framewise displacement of > 0.50 and denoised time series with DVARS > 1, where DVARS refers to BOLD signal rate of change between TRs) (88), poor temporal signal-to-noise ratio (< 50), or fewer than 10 retained BOLD-like components. Inspection of residual motion effects is detailed in *SI Appendix*. The denoised BOLD component coefficient sets in native space were then mapped to a common cortical surface (fsaverage5) in FreeSurfer and concatenated.

To examine age-related changes to functional brain network organization, we implemented a participant-specific functional parcellation approach with group prior individual parcellation (GPIP) (89). This approach initializes with a predefined group atlas (Schaefer 400) (42) and then, refines participants' parcel boundaries by drawing on their resting-state fMRI data. GPIP has been shown to improve the homogeneity of BOLD signal within parcels, better demarcate functional regions (89), and enhance the detection of brain-behavior associations (90, 91). The output of GPIP was a final optimal cortical parcellation for each participant from which BOLD coefficient sets were extracted.

In a separate analytical step, left and right anterior/posterior hippocampal regions of interest from ASHS were binarized and resampled to functional resolution in native space. BOLD coefficient sets were subsequently extracted with AFNI 3dmaskave (92–94) by run and concatenated.

Temporal Signal to Noise. The temporal signal-to-noise ratio, the mean signal intensity of a voxel divided by its SD across the time series, was calculated to assess scan quality. This ratio was calculated on three versions of the data (as in ref. 95) to illustrate the additive advantages of ME acquisitions and denoising (*SI Appendix*, Fig. S1): 1) a minimally preprocessed TE₂ as a proxy for single-echo data (*SI Appendix*, Fig. S1A), 2) the optimally combined ME data without denoising (*SI Appendix*, Fig. S1B), and 3) the ME denoised data used in the present report (*SI Appendix*, Fig. S1C). We quantified the temporal signal-to-noise ratio as the conjunction of gray matter and functional masks (76, 87) across the whole brain and within each hemisphere of AHIPP, PHIPP, and TP. The median of all voxels within these masks was used to characterize the quality of the BOLD signal for each participant for each run. For consistency across versions, here we use the FreeSurfer-defined TP instead of a parcellation-defined TP. Voxel-wise spatial maps were separately derived in standard MNI space across the whole brain for visualization (*SI Appendix*, Fig. S1 A, Left, B, Left, and C, Left). Maps were averaged across all participants and thresholded between 50 and 400 for all versions.

Functional Connectivity. To assess RSFC, we conducted a variation on seed-voxel connectivity between our three regions of interest—AHIPP, PHIPP, and TP—and an extended DN: LIM (LIM-A, LIM-B), default (DN-A, DN-B, DN-C), and TEMP-PAR subnetworks from the Yeo 17-network solution (32). LIM-A and LIM-B were included for TP and OFC parcels (ref. 33 has alternate subnetwork assignments). Fig. 1 shows a surface rendering and legend of subnetworks. Table 1 includes a full description of regions belonging to each subnetwork.

BOLD data were extracted from each participant's GPIP solution from only the parcels comprising these six subnetworks (119 parcels in total). Extracted BOLD data from AHIPP and PHIPP were added at this step. Functional connectivity matrices were then created by computing the product-moment (*r*) correlation coefficient between each pair of regions. A canonical Fisher's *r* to *z* transformation was applied (as in ref. 87) to simultaneously normalize the correlation values and account for varying degrees of freedom (i.e., the number of BOLD coefficients) across participants. The matrix of *z* values was then downsized to a rectangular 17 × 123 matrix to specifically examine how the BOLD signal in TP, AHIPP, and PHIPP covaried with LIM, DN, and TEMP-PAR subnetworks.

Analysis.

RSFC of AHIPP, PHIPP, and TP with the DN. Average RSFC was first calculated within each age group (Fig. 2B). Bootstrap resampling (resampling rate = 10,000) was used to calculate the 95% CI around each pairwise *z*-value connection and determine reliability. Connections with CIs crossing zero were masked out.

We performed a separate analysis to visualize the overall RSFC pattern of each region of interest with the extended DN across all participants (Fig. 2A). For each region of interest, BOLD data were averaged across parcels from both hemispheres, and RSFC matrices were recomputed, rendering three 1 × 109 matrices for each participant. The *z* values were averaged across all participants, and significance was determined with a one-sample *t* test. *P* values below 0.05 were masked out. AHIPP and PHIPP are not shown on the surface. For visualization purposes, all TP parcels in TP RSFC were assigned the maximum value in the matrix to indicate autocorrelation.

Age group differences in RSFC and relationships to AM. PLS was used to examine group differences in RSFC, and behavior PLS was used to examine RSFC associations with density scores from the Autobiographical Interview. PLS is a multivariate method that identifies patterns of maximal covariance between two sets of variables (96, 97). Here, those variables were represented by participant RSFC matrices and either 1) age group or 2) density scores.

To run PLS, a data matrix **X** was created with all participants' rectangular connectivity matrices. Each row of **X** corresponded to a vector containing one participant's within-network (LIM-A–LIM-A, AHIPP–AHIPP, PHIPP–PHIPP) and between-network connections. Column-wise means are then calculated by age group. All data in **X** were then mean centered and submitted to singular value decomposition to yield mutually orthogonal latent variables representing distinct relationships between the two variables mentioned above. Each latent variable consisted of 1) a left singular vector containing the weighted connectivity pattern optimally expressing the covariance, 2) a right singular vector with the weights of the study design variables (i.e., age group or density scores), and 3) a scalar singular value with the covariance strength between the design variable and connectivity. For each pattern, a brain connectivity score can be calculated from the dot product of the left singular vector (1) and each participant's functional connectivity matrix. Stronger positive values reflect expression of the warmer colors, while stronger negative values reflect expression of the cooler colors. Brain connectivity scores, therefore, represent the degree to which each participant expressed the pattern identified.

Permutation testing was used to statistically evaluate patterns identified, and bootstrap resampling determined the reliability of pairwise connections (1,000 permutations, 500 bootstraps). Connectivity weights were considered to significantly contribute to the overall pattern when bootstrap ratios (weight in the singular vector/bootstrap-estimated SE) exceeded ±1.96, corresponding to the 95% CI.

For display purposes, PLS results for each region of interest were mapped to the surface by averaging unthresholded results across parcels in the left and right hemispheres and then, thresholding to a bootstrap ratio of 1.96. AHIPP and PHIPP regions are not shown on the surface.

Partial correlations between brain connectivity scores and each region of interest volume (each hemisphere separately) were carried out to explore associations between volume and age group differences in RSFC. Covariates included sex, education, eWBV, and framewise displacement. Associations were considered significant at *P* < 0.05. Site was not included as a covariate since participants across sites added desirable variability due to increased demographic diversity in the Toronto cohort (*SI Appendix*). Instead, we ensured that any age group effects existed over and above site effects by conducting analyses of covariance on brain connectivity scores with site, sex, education, eWBV, and mean framewise displacement as covariates [*F*(1,256) = 78.60, *P* < 0.001, $\eta_p^2 = 0.23$]. Correlations with site included as a covariate are also reported for completeness. We also report partial correlations between brain connectivity scores from behavior PLS and density scores with sex, education, eWBV, framewise displacement, and site as covariates with the corresponding results.

A final set of post hoc correlations was conducted between brain connectivity scores from behavior PLS and more granular detail categories. The goal was to explore which specific detail types contributed to associations between RSFC and internal/external density (i.e., internal: event, place, time, perceptual, emotion/thought details; external: semantic, repetition, other, event, place, time, perceptual, emotion/thought). Partial correlations were run between brain connectivity scores and detail density from all detail categories with sex, education, eWBV, and

framework displacement as covariates. Results with site as an additional covariate are also provided. Associations were considered significant at $P < 0.05$.

Network contributions. PLS identifies interregional connectivity patterns that differ by group and/or covary with density scores. To examine network-level effects for each analysis, we calculated network contributions to each PLS-derived functional connectivity pattern (28, 91). Positive and negative weighted adjacency matrices were constructed from the PLS pattern; nodes represented parcels defined by either the individual parcellation or a unilateral segment of the hippocampus (i.e., left AHIPP), while edges represented the thresholded bootstrap ratio of each pairwise connection. Network-level contributions were then quantified by 1) assigning each parcel according to the network assignment reported by Yeo et al. (32) or to a hippocampal "network" (left and right AHIPP, left and right PHIPP), 2) taking the average of all connection weights in a given network and calculating within- and between-network connectivity to yield a 3×8 matrix (LIM-A, AHIPP, PHIPP \times LIM-A, LIM-B, DN-A, DN-B, DN-C, TEMP-PAR, AHIPP, PHIPP), and 3) permutation testing for significance. For each of 10,000 permutations, network labels were shuffled, and mean within- and between-network connectivity estimates were recalculated. After 10,000 iterations, an empirical null sampling distribution was created. Within- and between-network connections were deemed significant when the proportion of times the value of the

sampling distribution was greater than or equal to the empirical value did not exceed 0.05 (Fig. 1 shows an example).

Data, Materials, and Software Availability. Behavioral data have been deposited in the Open Science Framework (<https://doi.org/10.17605/OSF.IO/YHZXE>) (98), and neuroimaging data have been deposited in OpenNeuro (<https://doi.org/10.18112/openneuro.ds003592.v1.0.3>) (99).

ACKNOWLEDGMENTS. This project was supported in part by a grant from the Canadian Institutes of Health Research (to R.N.S.) and NIH Grant 1S10RR025145. The authors would like to thank Karen L. Campbell for feedback on an earlier version of the manuscript.

Author affiliations: ^aDepartment of Psychology, Harvard University, Cambridge, MA, 02138; ^bMontreal Neurological Institute, Department of Neurology and Neurosurgery, McGill University, Montreal, QC, H3A 2B4, Canada; ^cDepartment of Psychology, McGill University, Montreal, QC, H3A 1G1, Canada; ^dDepartment of Psychology, York University, Toronto, ON, M3J 1P3, Canada; ^eMcConnell Brain Imaging Centre, McGill University, Montreal, QC, H3A 2B4, Canada; ^fDepartment of Psychiatry, McGill University, Montreal, QC, H3A 1A1, Canada; and ^gDouglas Mental Health Institute, Verdun, QC, H4H 1R3, Canada

1. D. J. Palombo, S. Sheldon, B. Levine, Individual differences in autobiographical memory. *Trends Cogn. Sci.* **22**, 583–597 (2018).
2. B. Levine, E. Svoboda, J. F. Hay, G. Winocur, M. Moscovitch, Aging and autobiographical memory: Dissociating episodic from semantic retrieval. *Psychol. Aging* **17**, 677–689 (2002).
3. P. J. Eslinger, Autobiographical memory after temporal lobe lesions. *Neurocase* **4**, 481–495 (1998).
4. K. Herfurth, B. Kasper, M. Schwarz, H. Stefan, E. Pauli, Autobiographical memory in temporal lobe epilepsy: Role of hippocampal and temporal lateral structures. *Epilepsy Behav.* **19**, 365–371 (2010).
5. M. Irish, O. Piguet, The pivotal role of semantic memory in remembering the past and imagining the future. *Front. Behav. Neurosci.* **7**, 27 (2013).
6. E. Svoboda, M. C. McKinnon, B. Levine, The functional neuroanatomy of autobiographical memory: A meta-analysis. *Neuropsychologia* **44**, 2189–2208 (2006).
7. R. N. Spreng, R. A. Mar, A. S. Kim, The common neural basis of autobiographical memory, prospection, navigation, theory of mind, and the default mode: A quantitative meta-analysis. *J. Cogn. Neurosci.* **21**, 489–510 (2009).
8. M. D. Rugg, K. L. Vilberg, Brain networks underlying episodic memory retrieval. *Curr. Opin. Neurobiol.* **23**, 255–260 (2013).
9. R. G. Benoit, D. L. Schacter, Specifying the core network supporting episodic simulation and episodic memory by activation likelihood estimation. *Neuropsychologia* **75**, 450–457 (2015).
10. Z. M. Reagh, C. Ranganath, What does the functional organization of cortico-hippocampal networks tell us about the functional organization of memory? *Neurosci. Lett.* **680**, 69–76 (2018).
11. M. Ritchey, R. A. Cooper, Deconstructing the posterior medial episodic network. *Trends Cogn. Sci.* **24**, 451–465 (2020).
12. S. Sheldon, B. Levine, The role of the hippocampus in memory and mental construction. *Ann. N. Y. Acad. Sci.* **1369**, 76–92 (2016).
13. J. R. Andrews-Hanna, J. Smallwood, R. N. Spreng, The default network and self-generated thought: Component processes, dynamic control, and clinical relevance. *Ann. N. Y. Acad. Sci.* **1316**, 29–52 (2014).
14. C. Ranganath, M. Ritchey, Two cortical systems for memory-guided behaviour. *Nat. Rev. Neurosci.* **13**, 713–726 (2012).
15. J. R. Andrews-Hanna, M. D. Grilli, M. Irish, "A review and reappraisal of the default network in normal aging and dementia" in *Oxford Research Encyclopedia of Psychology*, B. G. Knight, Ed., (Oxford University Press, 2019), pp. 1–32.
16. D. L. Schacter et al., The future of memory: Remembering, imagining, and the brain. *Neuron* **76**, 677–694 (2012).
17. J. S. Damoiseaux, Effects of aging on functional and structural brain connectivity. *Neuroimage* **160**, 32–40 (2017).
18. K. L. Campbell, O. Grigg, C. Saverino, N. Churchill, C. L. Grady, Age differences in the intrinsic functional connectivity of default network subsystems. *Front. Aging Neurosci.* **5**, 73 (2013).
19. W. D. Stevens, R. N. Spreng, Resting-state functional connectivity MRI reveals active processes central to cognition. *Wiley Interdiscip. Rev. Cogn. Sci.* **5**, 233–245 (2014).
20. S. Sheldon, N. Farb, D. J. Palombo, B. Levine, Intrinsic medial temporal lobe connectivity relates to individual differences in episodic autobiographical remembering. *Cortex* **74**, 206–216 (2016).
21. R. Petrican, D. J. Palombo, S. Sheldon, B. Levine, The neural dynamics of individual differences in episodic autobiographical memory. *eNeuro* **7**, ENEURO.0531-19.2020 (2020).
22. S. Matijevic, J. R. Andrews-Hanna, A. A. Wank, L. Ryan, M. D. Grilli, Individual differences in the relationship between episodic detail generation and resting state functional connectivity vary with age. *Neuropsychologia* **166**, 108138 (2022).
23. I. Kahn, J. R. Andrews-Hanna, J. L. Vincent, A. Z. Snyder, R. L. Buckner, Distinct cortical anatomy linked to subregions of the medial temporal lobe revealed by intrinsic functional connectivity. *J. Neurophysiol.* **100**, 129–139 (2008).
24. M. Moscovitch, R. Cabeza, G. Winocur, L. Nadel, Episodic memory and beyond: The hippocampus and neocortex in transformation. *Annu. Rev. Psychol.* **67**, 105–134 (2016).
25. R. A. Cooper, M. Ritchey, Cortico-hippocampal network connections support the multidimensional quality of episodic memory. *eLife* **8**, e45591 (2019).
26. P. Kundu et al., Multi-echo fMRI: A review of applications in fMRI denoising and analysis of BOLD signals. *Neuroimage* **154**, 59–80 (2017).
27. L. Raimondo et al., Advances in resting state fMRI acquisitions for functional connectomics. *Neuroimage* **243**, 118503 (2021).
28. R. Setton et al., Age differences in the functional architecture of the human brain. *Cereb. Cortex*, 10.1093/cercor/bhac056 (2022).
29. R. M. Braga, R. L. Buckner, Parallel interdigitated distributed networks within the individual estimated by intrinsic functional connectivity. *Neuron* **95**, 457–471.e5 (2017).
30. S. Sheldon, C. Fenerci, L. Gurguryan, A neurocognitive perspective on the forms and functions of autobiographical memory retrieval. *Front. Syst. Neurosci.* **13**, 4 (2019).
31. A. W. Lockrow et al., Taking stock of the past: A comprehensive psychometric evaluation of the autobiographical interview. bioRxiv [Preprint] (2021). <https://www.biorxiv.org/content/10.1101/2021.12.22.473803v1> (Accessed 23 December 2021).
32. B. T. Yeo et al., The organization of the human cerebral cortex estimated by intrinsic functional connectivity. *J. Neurophysiol.* **106**, 1125–1165 (2011).
33. R. Kong et al., Individual-specific areal-level parcellations improve functional connectivity prediction of behavior. *Cereb. Cortex* **31**, 4477–4500 (2021).
34. R. N. Spreng, W. D. Stevens, J. D. Viviano, D. L. Schacter, Attenuated anticorrelation between the default and dorsal attention networks with aging: Evidence from task and rest. *Neurobiol. Aging* **45**, 149–160 (2016).
35. R. Setton, S. Sheldon, G. R. Turner, R. N. Spreng, Temporal pole volume is associated with episodic autobiographical memory in healthy older adults. *Hippocampus* **32**, 373–385 (2022).
36. A. Salami, A. Wählin, N. Kaboodvand, A. Lundquist, L. Nyberg, Longitudinal evidence for dissociation of anterior and posterior MTL resting-state connectivity in aging: Links to perfusion and memory. *Cereb. Cortex* **26**, 3953–3963 (2016).
37. S. M. Stark, A. Frithsen, C. E. L. Stark, Age-related alterations in functional connectivity along the longitudinal axis of the hippocampus and its subfields. *Hippocampus* **31**, 11–27 (2021).
38. J. S. Damoiseaux, R. P. Viviano, P. Yuan, N. Raz, Differential effect of age on posterior and anterior hippocampal functional connectivity. *Neuroimage* **133**, 468–476 (2016).
39. M. Y. Chan, D. C. Park, N. K. Savalia, S. E. Petersen, G. W. Sig, Decreased segregation of brain systems across the healthy adult lifespan. *Proc. Natl. Acad. Sci. U.S.A.* **111**, E4997–E5006 (2014).
40. L. Geerligns, R. J. Renken, E. Saliassi, N. M. Maurits, M. M. Lorst, A brain-wide study of age-related changes in functional connectivity. *Cereb. Cortex* **25**, 1987–1999 (2015).
41. J. R. Andrews-Hanna, J. S. Reidler, J. Sepulcre, R. Poulin, R. L. Buckner, Functional-anatomic fractionation of the brain's default network. *Neuron* **65**, 550–562 (2010).
42. A. Schaefer et al., Local-global parcellation of the human cerebral cortex from intrinsic functional connectivity MRI. *Cereb. Cortex* **28**, 3095–3114 (2018).
43. R. M. Braga, L. M. DiNicola, H. C. Becker, R. L. Buckner, Situating the left-lateralized language network in the broader organization of multiple specialized large-scale distributed networks. *J. Neurophysiol.* **124**, 1415–1448 (2020).
44. Z. Mineroff, I. A. Blank, K. Mahowald, E. Fedorenko, A robust dissociation among the language, multiple demand, and default mode networks: Evidence from inter-region correlations in effect size. *Neuropsychologia* **119**, 501–511 (2018).
45. E. T. Rolls, G. Deco, C.-C. Huang, J. Feng, The human language effective connectome. *Neuroimage* **258**, 119352 (2022).
46. X. Blaizot et al., The human parahippocampal region. I. Temporal pole cytoarchitectonic and MRI correlation. *Cereb. Cortex* **20**, 2198–2212 (2010).
47. A. S. Persichetti, J. M. Denning, S. J. Gotts, A. Martin, A data-driven functional mapping of the anterior temporal lobes. *J. Neurosci.* **41**, 6038–6049 (2021).
48. A. Zheng et al., Parallel hippocampal-parietal circuits for self- and goal-oriented processing. *Proc. Natl. Acad. Sci. U.S.A.* **118**, e2101743118 (2021).
49. D. C. Park, P. Reuter-Lorenz, The adaptive brain: Aging and neurocognitive scaffolding. *Annu. Rev. Psychol.* **60**, 173–196 (2009).
50. M. Y. Chan et al., Socioeconomic status moderates age-related differences in the brain's functional network organization and anatomy across the adult lifespan. *Proc. Natl. Acad. Sci. U.S.A.* **115**, E5144–E5153 (2018).
51. D. R. Addis, R. P. Roberts, D. L. Schacter, Age-related neural changes in autobiographical remembering and imagining. *Neuropsychologia* **49**, 3656–3669 (2011).
52. A. Viard et al., Hippocampal activation for autobiographical memories over the entire lifetime in healthy aged subjects: An fMRI study. *Cereb. Cortex* **17**, 2453–2467 (2007).

53. P. Martinelli *et al.*, Age-related changes in the functional network underlying specific and general autobiographical memory retrieval: A pivotal role for the anterior cingulate cortex. *PLoS One* **8**, e82385 (2013).
54. C. Fenerci, L. Gurguryan, R. N. Spreng, S. Sheldon, Comparing neural activity during autobiographical memory retrieval between younger and older adults: An ALE meta-analysis. *Neurobiol. Aging* **119**, 8–21 (2022).
55. A. Adnan *et al.*, Distinct hippocampal functional networks revealed by tractography-based parcellation. *Brain Struct. Funct.* **221**, 2999–3012 (2016).
56. F. J. Calabro, V. P. Murty, M. Jalbrzikowski, B. Tervo-Clemmens, B. Luna, Development of hippocampal-prefrontal cortex interactions through adolescence. *Cereb. Cortex* **30**, 1548–1558 (2020).
57. V. P. Murty, F. Calabro, B. Luna, The role of experience in adolescent cognitive development: Integration of executive, memory, and mesolimbic systems. *Neurosci. Biobehav. Rev.* **70**, 46–58 (2016).
58. C. McCormick, M. St-Laurent, A. Ty, T. A. Valiante, M. P. McAndrews, Functional and effective hippocampal-neocortical connectivity during construction and elaboration of autobiographical memory retrieval. *Cereb. Cortex* **25**, 1297–1305 (2015).
59. A. Gilboa, H. Marlatte, Neurobiology of schemas and schema-mediated memory. *Trends Cogn. Sci.* **21**, 618–631 (2017).
60. C. McCormick, D. N. Barry, A. Jafarian, G. R. Barnes, E. A. Maguire, vmPFC drives hippocampal processing during autobiographical memory recall regardless of remoteness. *Cereb. Cortex* **30**, 5972–5987 (2020).
61. M. A. Ralph, E. Jefferies, K. Patterson, T. T. Rogers, The neural and computational bases of semantic cognition. *Nat. Rev. Neurosci.* **18**, 42–55 (2017).
62. P. P. Raykov, J. L. Keidel, J. Oakhill, C. M. Bird, The importance of semantic network brain regions in integrating prior knowledge with an ongoing dialogue. *bioRxiv* [Preprint] (2021). <https://www.biorxiv.org/content/10.1101/276683v3> (Accessed 1 October 2021).
63. P. Piolino, B. Desgranges, K. Benali, F. Eustache, Episodic and semantic remote autobiographical memory in ageing. *Memory* **10**, 239–257 (2002).
64. A. Gazzaley, J. W. Cooney, J. Rissman, M. D'Esposito, Top-down suppression deficit underlies working memory impairment in normal aging. *Nat. Neurosci.* **8**, 1298–1300 (2005).
65. C. Strikwerda-Brown, A. Mothakunnel, J. R. Hodges, O. Piquet, M. Irish, External details revisited: A new taxonomy for coding 'non-episodic' content during autobiographical memory retrieval. *J. Neuropsychol.* **13**, 371–397 (2019).
66. I. R. Olson, A. Plotzker, Y. Ezyat, The Enigmatic temporal pole: A review of findings on social and emotional processing. *Brain* **130**, 1718–1731 (2007).
67. M. A. Conway, C. W. Pleydell-Pearce, The construction of autobiographical memories in the self-memory system. *Psychol. Rev.* **107**, 261–288 (2000).
68. K. L. Campbell, D. L. Schacter, Aging and the resting state: Is cognition obsolete? *Lang. Cogn. Neurosci.* **32**, 661–668 (2017).
69. E. S. Finn, Is it time to put rest to rest? *Trends Cogn. Sci.* **25**, 1021–1032 (2021).
70. J. Robin, M. Moscovitch, Details, gist and schema: Hippocampal-neocortical interactions underlying recent and remote episodic and spatial memory. *Curr. Opin. Behav. Sci.* **17**, 114–123 (2017).
71. L. Geerligns, K. A. Tsvetanov, Cam-Can, R. N. Henson, Challenges in measuring individual differences in functional connectivity using fMRI: The case of healthy aging. *Hum. Brain Mapp.* **38**, 4125–4156 (2017).
72. A. W. Gilmore *et al.*, Dynamic content reactivation supports naturalistic autobiographical recall in humans. *J. Neurosci.* **41**, 153–166 (2021).
73. A. T. Beck, R. A. Steer, G. K. Borwn, *Manual for the Beck Depression Inventory-II* (Psychological Corporation, 1996).
74. J. A. Yesavage *et al.*, Development and validation of a geriatric depression screening scale: A preliminary report. *J. Psychiatr. Res.* **17**, 37–49 (1982-1983).
75. M. F. Folstein, S. E. Folstein, P. R. McHugh, "Mini-mental state": A practical method for grading the cognitive state of patients for the clinician. *J. Psychiatr. Res.* **12**, 189–198 (1975).
76. R. N. Spreng *et al.*, Neurocognitive aging data release with behavioral, structural and multi-echo functional MRI measures. *Sci. Data* **9**, 119 (2022).
77. B. Fischl *et al.*, Whole brain segmentation: Automated labeling of neuroanatomical structures in the human brain. *Neuron* **33**, 341–355 (2002).
78. M. Reuter, N. J. Schmansky, H. D. Rosas, B. Fischl, Within-subject template estimation for unbiased longitudinal image analysis. *Neuroimage* **61**, 1402–1418 (2012).
79. P. A. Yushkevich *et al.*, Automated volumetry and regional thickness analysis of hippocampal subfields and medial temporal cortical structures in mild cognitive impairment. *Hum. Brain Mapp.* **36**, 258–287 (2015).
80. L. Xie *et al.*, Accounting for the confound of meninges in segmenting entorhinal and perirhinal cortices in T1-weighted MRI. *Med. Image Comput. Comput. Assist. Interv.* **9901**, 564–571 (2016).
81. L. Zajac *et al.*, Hippocampal resting-state functional connectivity patterns are more closely associated with severity of subjective memory decline than whole hippocampal and subfield volumes. *Cereb. Cortex Commun.* **1**, tga0019 (2020).
82. J. Poppenk, M. Moscovitch, A hippocampal marker of recollection memory ability among healthy young adults: Contributions of posterior and anterior segments. *Neuron* **72**, 931–937 (2011).
83. C. R. Jack Jr. *et al.*, Anterior temporal lobes and hippocampal formations: Normative volumetric measurements from MR images in young adults. *Radiology* **172**, 549–554 (1989).
84. R. L. Buckner *et al.*, A unified approach for morphometric and functional data analysis in young, old, and demented adults using automated atlas-based head size normalization: Reliability and validation against manual measurement of total intracranial volume. *Neuroimage* **23**, 724–738 (2004).
85. S. M. Smith, Fast robust automated brain extraction. *Hum. Brain Mapp.* **17**, 143–155 (2002).
86. P. Kundu, S. J. Inati, J. W. Evans, W. M. Luh, P. A. Bandettini, Differentiating BOLD and non-BOLD signals in fMRI time series using multi-echo EPI. *Neuroimage* **60**, 1759–1770 (2012).
87. P. Kundu *et al.*, Integrated strategy for improving functional connectivity mapping using multiecho fMRI. *Proc. Natl. Acad. Sci. U.S.A.* **110**, 16187–16192 (2013).
88. J. D. Power, K. A. Barnes, A. Z. Snyder, B. L. Schlaggar, S. E. Petersen, Spurious but systematic correlations in functional connectivity MRI networks arise from subject motion. *Neuroimage* **59**, 2142–2154 (2012).
89. M. Chong *et al.*, Individual parcellation of resting fMRI with a group functional connectivity prior. *Neuroimage* **156**, 87–100 (2017).
90. R. Kong *et al.*, Spatial topography of individual-specific cortical networks predicts human cognition, personality, and emotion. *Cereb. Cortex* **29**, 2533–2551 (2019).
91. L. Mwilambwe-Tshilobo *et al.*, Loneliness and meaning in life are reflected in the intrinsic network architecture of the brain. *Soc. Cogn. Affect. Neurosci.* **14**, 423–433 (2019).
92. R. W. Cox, AFNI: Software for analysis and visualization of functional magnetic resonance neuroimages. *Comput. Biomed. Res.* **29**, 162–173 (1996).
93. R. W. Cox, J. S. Hyde, Software tools for analysis and visualization of fMRI data. *NMR Biomed.* **10**, 171–178 (1997).
94. S. Gold *et al.*, Functional MRI statistical software packages: A comparative analysis. *Hum. Brain Mapp.* **6**, 73–84 (1998).
95. J. Gonzalez-Castillo *et al.*, Evaluation of multi-echo ICA denoising for task based fMRI studies: Block designs, rapid event-related designs, and cardiac-gated fMRI. *Neuroimage* **141**, 452–468 (2016).
96. A. R. McIntosh, N. J. Lobaugh, Partial least squares analysis of neuroimaging data: Applications and advances. *Neuroimage* **23** (suppl. 1), S250–S263 (2004).
97. A. R. McIntosh, B. Misić, Multivariate statistical analyses for neuroimaging data. *Annu. Rev. Psychol.* **64**, 499–525 (2013).
98. R. N. Spreng, Goal-directed cognition in older and younger adults. Open Science Framework. <https://doi.org/10.17605/OSF.IO/YHZXE>. Deposited 11 December 2020.
99. R. N. Spreng *et al.*, Neurocognitive data release with behavioral, structural, and multi-echo functional MRI measures. OpenNeuro. <https://doi.org/10.18112/openneuro.ds003592.v1.0.3>. Deposited 29 March 2021.